Taylor & Francis
Taylor & Francis Group

Effect of methyl methacrylate concentrations on surface and thermal analysis of composite polymer polymethylmethacrylates with mesogen reactive RM82

Afrizal [ID][a], Yusmaniar[a], Bryan Valentino[a], Asep Riswoko[b] and Karin Khairunnisa Gumilar[a]

[a]Department of Chemistry, Faculty of Mathematics and Natural Sciences, Universitas Negeri Jakarta, Jakarta, Indonesia; [b]National Research and Innovation Agency, KST Habibie, South Tangerang, Indonesia

ABSTRACT

This research report of the synthesis of composite polymers from liquid crystal mesogen reactive (RM82) monomers with Methyl methacrylate (MMA). The purpose of this research is analysis the effect concentration of MMA on the surface and thermal of the composite polymer PMMA-RM82. The result of the morphological analysis of composite surfaces performed by polarization optical microscopy (POM) technique showed liquid crystal textures affected composition from two monomers. SEM images show that the surface of the RM82 liquid crystal has a shape resembling fibrous and blade-like crystals with a length of up to 10 μm (micrometers). Analysis thermal showed the heat released by the PMMA-RM82 increased with the increase in MMA weight percent. This affects the rapid crystallization process of PMMA-RM82 which of concentration MMA 30%-RM82 the heat released is almost twice as much as the heat released by MMA 5%-RM82. The absence of PMMA and RM82 peaks both endothermic and exothermic in PMMA-RM82 samples indicates that polymerization has occurred and a new product has formed. Analysis structure molecule by FTIR found that the IR spectral form of each variation in the weight percent of MMA was almost the same, but there was a spectral shift that showed that polymerization had occurred in PMMA-RM82 which was characterized by a reaction to the free radical C=C bond released by the photoinitiator. XRD pattern of composite PMMA-RM82 showed the peaks formed are located at scattering angles similar to RM82 but there is a decrease in intensity as the percent weight of MMA increases.

1. Introduction

Polymer research has undergone significant improvements in several areas, namely new material synthesis research, high polymer performance studies, and breakthrough applications of polymer materials in several fields, thus encouraging the development of newer and better polymerization research. One of the developments in polymer research is the study of liquid crystal polymers. This is comparable to the applications of crystalline polymers in a variety of fields. The uses of liquid crystal polymers are numerous in areas ranging from laser beam deflectors, automotive parts, aerospace, and food containers to monofilament fibers [1,2].

The research and development of composite polymers has led to the creation of smart materials. Monomer liquid crystals can be combined with other types of polymers. This research uses a thermoplastic-type polymer methyl methacrylate. According to references, polymethyl methacrylate (PMMA) is widely used because it is easy to obtain and has high stability to chemicals and weather [3,4]. Liquid

crystal monomers that are usually used in the synthesis of composite polymers are types of reactive mesogenous compounds. The reactive mesogen liquid crystal monomer that can be used is RM82. Reactive mesogen combined with material of monomer polymethylmetacrylate will produce porous composite materials [5,6]. The research novelty lies in the introduction of RM82, which can be combined with other monomers to produce composite polymers. Polymerization of both monomers is easy, requiring few reagents and resulting in zero waste.

The liquid crystal monomer used in this research is the molecular structure of RM82, which is a reactive final group and can polymerize each other under ultraviolet light. Another advantage is that reactive mesogens exhibit liquid crystal properties, i.e., self-assembly, dielectric properties, and anisotropic optics. Product polymer composites from MMA polymers with RM82 have the potential to become membranes. This is based on previous research that explains the possibility of liquid crystal polymers becoming membranes [7,8].

The properties of PMMA enable it to serve as a matrix in the composite formation process [9,10]. Based on the results of this study, the ability of PMMA to form a composite with RM82 was observed. PMMA concentration will have a great influence on the formation of the composite. Therefore, this study aims to investigate the influence of PMMA concentration on the formation of PMMA-RM 82 composites.

2. Materials and methods

2.1. Materials

The ingredients used in this study were MMA, dimethylformamide (DMF), chloroform ($CHCl_3$), aqua DM (demineralized), benzoyl peroxide, and reactive mesogen RM82. The tools used in this study were a set of glass tools, a *hotplate stirrer*, a glass plate, and a set of UV curing tools. The method used in this study is an experimental method, which consists of PMMA-RM82 liquid crystal polymer synthesis with the modification of PMMA weight percent composition and sample characterization with DSC (differential scanning calorimetry), FTIR (Fourier transform infrared), SEM (scanning electron microscopy), and XRD (X-ray diffraction). The information regarding the materials used in this research is as follows: chloroform: Purity 99.0–99.4%, manufactured by Sigma-Aldrich Pte-Ltd, Germany. Benzoyl peroxide: Purity 70–<90%, manufactured by Merck KGaA, Germany. MMA: Purity = 99%, manufactured by Merck KGaA, Germany. DMF: Purity = 99.8%, manufactured by Sigma-Aldrich Pte Ltd, Germany. RM82: Purity 95%, manufactured by Tokyo Chemical Industry Co., Ltd, Japan.

2.2. Methods

Composites this research were prepared by mixing the monomer MMA with the monomer liquid crystal RM82. Compositions were MMA with weight percent variations of 5% (1.9 g), 10% (1.8 g), 20% (1.6 g), and 30% (1.4 g), dissolved in a DMF-Chloroform cosolvent solution with a ratio of w/w 7:3, with dissolving conditions at room temperature and a stirrer speed of 20 rpm for 10 minutes. Therefore, for all variations of MMA, the use of the monomer RM82 was 30% (1.4 g). The formed solution is then mixed with RM82 reactive mesogen and benzoyl peroxide initiator. It is then stirred at 60°C with a stirrer speed of 200 rpm for 5 minutes to form a transparent PMMA-RM82 solution. The formed solution is then poured onto a glass plate to be polymerized using a UV curing tool for 10 minutes. The formed samples were then characterized using DSC, FTIR, SEM, and XRD. The information regarding the instruments utilized for the analysis of composite polymer PMMA-RM82 is as follows: FTIR: Bruker Alpha II (Bruker Optics, Germany), SEM: Zeiss EVO MA10 (Carl Zeiss, Germany), XRD: Empyrean Series 3 (Malvern Panalytical, UK), and DSC: DSC-60 (Shimadzu, Japan).

3. Results and discussion

The manufacturing process of PMMA-RM 82 composite involves a polymerization process with the mechanism of extending each monomer chain into a polymer chain. Both PMMA and RM82 monomers have acrylate groups that can undergo chain elongation or propagation reactions. Therefore, the two monomers have the same polymerization mechanism, namely addition polymerization. Consequently, the composite formation process with photopolymerization techniques will form polymers that have interrelated polymer chains between the two polymers. According to references, the combination of two monomers that undergo polymerization may form a cross-linking chain or a three-dimensional network [11–13]. However, this occurrence depends on many factors [10,12,14].

Liquid crystal recitative mesogen RM82 is a monomer that also has the ability to undergo addition polymerization process. Therefore, the merging of MMA with RM82 would be an interesting polymerization process, namely between the monomers themselves and also between the two monomers. According to the literature, the addition polymerization process, also known as free radical polymerization, consists of initiation, propagation, and termination stages. At the initiation stage, the initiator benzoyl peroxide undergoes homolytic breaking at high temperatures, producing benzoyl radicals. Furthermore, at the propagation stage, the benzoyl radical attacks the reactive mesogen monomer RM82 and MMA monomer, and it is expected that the two monomers combine to form a long chain of polymers. The propagation reaction lasts until the composition of each monomer is exhausted and then the termination process occurs in the form of the formation of bonds between mesogen and PMMA polymers [15,16].

In general, the polymerization process is described in Figure 1(a–d). Figure 1(a–d) illustrate the polymerization process between MMA monomers and RM82. The first stage of the BPO initiator undergoes a process of becoming radicalized which will then attack MMA monomers and RM82 monomers eventually each monomer becomes a radical monomer and propagates each other to carry out the chain extension process.

Composites in this research were prepared by mixing the monomer MMA with the monomer liquid crystal RM82. Compositions were MMA with weight percent
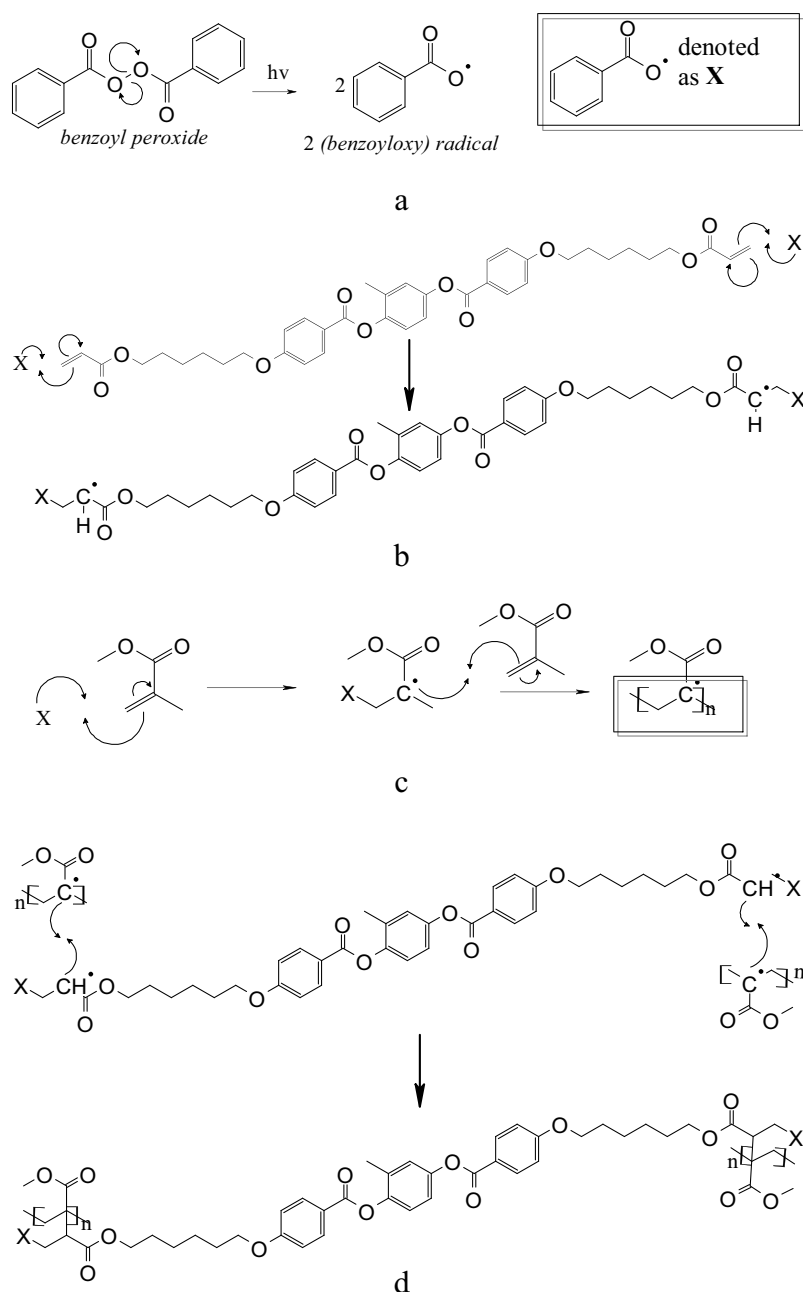
Figure 1. (a) Polymerization of initiator benzoyl peroxide. (b) Propagations mechanism of RM82. (c) Propagations mechanism of MMA. (d)Termination process of polymerization of MMA and RM82.

variations of 5%, 10%, 20%, and 30%, dissolved in a DMF-Chloroform *cosolvent* solution with a ratio of w/w 7:3, with dissolving conditions at room temperature and a stirrer speed of 20 rpm for 10 minutes. Therefore, for all variations of MMA, the use of the monomer RM82 was 30%. The photopolymerization process is performed for 10 minutes using UV curing, that photopolymerization conditions (weight monomers) about a short time. Photopolymerization process using benzoyl peroxide initiator and UV light. Therefore in UV curing process about a short time.

Polymerization between MMA monomer and RM82 will form a very complex polymer chain, commonly referred to as an elastomer [17,18]. Based on the results of this study, it is expected that the elastomer produced will be maximized at the time of application. Liquid crystal monomer elastomers will generally have many advantages as materials with many benefits [19].

Analysis using a polarization optical microscope (POM) was conducted on polymer composite of PMMA-RM82 to explore liquid crystal properties of RM82 on composite polymer. Images captured via POM of the

composite in variations of concentration of MMA can be seen in Figure 2. In general, the morphology of the thin-layer film produced from the PMMA-RM82 polymer composite after the UV curing process appears transparent. However, after 24 hours of storage, it can be seen that there are parts that were initially transparent to form an opaque surface.

Morphological analysis of composite surfaces is performed using polarization optical microscopy, which showed the effect of MMA concentration. As depicted in Figure 2, the composite from 5% MMA is transparent and clear colour of liquid crystal RM82 and this images for 10% MMA. Therefore, after added MMA are 20% and 30%, morphology of composites changes be blue and opaque. These conditions explained that MMA much more blend to composite and liquid crystal effect decrease [20].

Morphological analysis of the PMMA-RM82 composite using SEM was performed with a secondary electron detector and an electron energy of 20 kV, with a photomagnification of 2500×. Morphological images of the composite SEM results can be seen in Figure 3.

Based on the SEM images in Figure 3, it can be seen that the surface of the RM82 liquid crystal has fibrous and blade-like crystals with lengths of up to 10 µm (micrometers). This sample is an aggregate of high-molecular weight. Upon adding PMMA, with a PMMA weight percent of 5%, a new shape emerges in the form of a large circle attached to the end of the blade, as seen in Figure 3b [21–23]. This indicates that polymerization

began to occur in PMMA-RM82. That the peak of PMMA weight gain of 30% occurred cross-linking *aggregation* which resulted in a change in shape to become like a crystal chunk indicating that a phase had formed in the product [24–26].

Composite thermal analysis of PMMA-RM82 was conducted using a heat-flux-type DSC instrument in the temperature range of 30–300°C for 30 min under N_2 atmosphere, as shown in Figure 4. In *DSC heat flux*, endothermic activity causes the sample to absorb heat and must be cooler than the furnace, so the peak points downward, also known as *endo down*. While in *heat flow* DSC, the same activity requires the instrument to supply more power to the sample so that the sample temperature and reference are maintained at the same temperature, so the endothermic peak points up, also known as *endo up* [27,28].

In the RM82 sample, the resulting DSC curve only has small endothermic peaks and are not very sharp, while in the DSC curve, PMMA-RM82 exhibits sharp endothermic and exothermic peaks, as shown in Figures 5 and 6. This indicates that thermal transformation activity at RM82 tends to be slow with a small enthalpy change at peak, whereas after the addition of PMMA at a certain weight percent, there is a rapid thermal transformation activity, with a large enthalpy change compared to enthalpy change without PMMA addition [29].

The RM82 thermogram has a low melting point curve (Tm) compared to other PMMA-RM82 composites. This illustrates that the melting process in composite polymers requires higher temperatures because they have
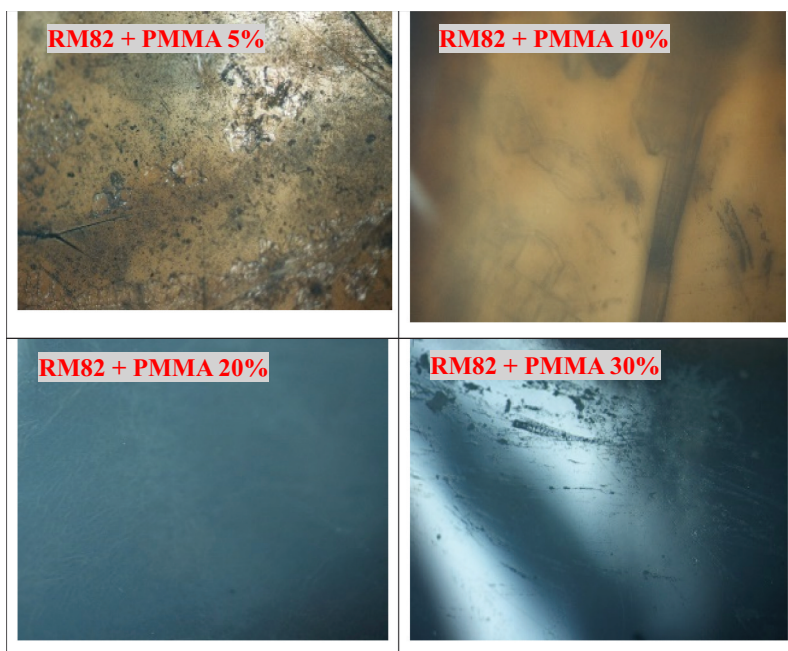

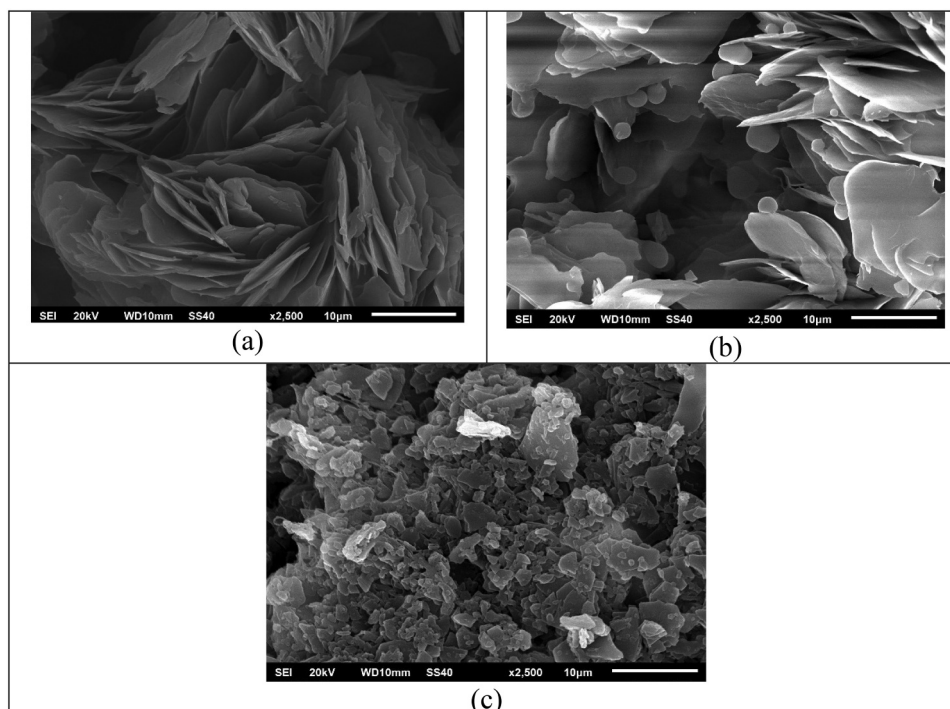**Figure 2.** POM images of composites of PMMA-RM82.

Figure 3. SEM images of composite: (a) RM82, (b) PMMA 5% – RM82, and (c) PMMA 30% – RM82.
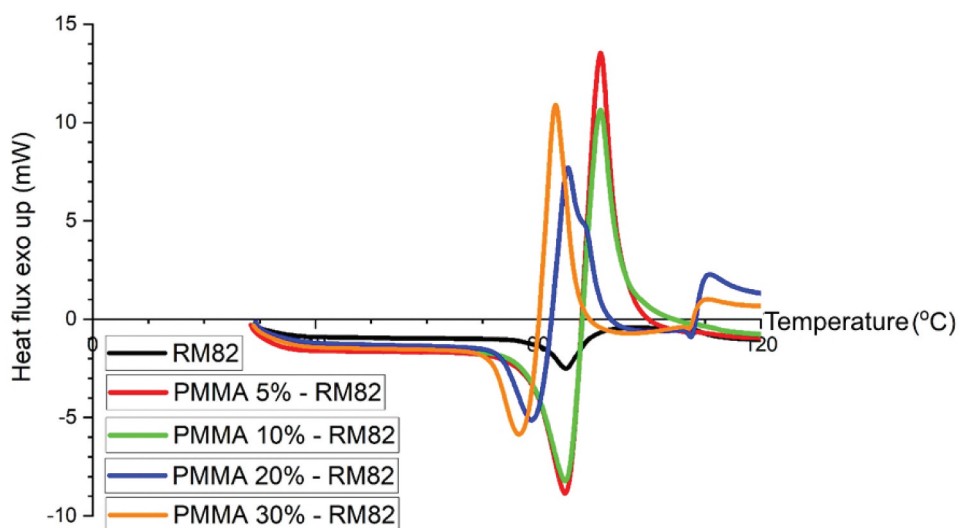

Figure 4. Thermogram DSC of PMMA-RM82.

undergone a crystallization process or cross-linking bonds in the PMMA-RM82 polymer composite that is formed. On the thermogram, it can also be seen that the PMMA-RM82 composite exothermic peak is very sharp. This indicates the crystallization process formed in the composite. The addition of monomers to RM82 forms polymer composites that form crystalline phases in the polymer more and more. Where a cross-linking curve is formed on the PMMA-RM82 composite, it indicates the occurrence of a 'cure' process. Thus, it can be said that the cure or cross-link process occurred in this study.

The difference in melting and crystallization temperature peaks is due to the variation in composition of each sample, although the mixture is the same. The results of this study show that the composition of PMMA-RM82 with variations in MMA composition will provide different thermal properties as well. This is because the composite polymer chains formed vary depending on the composition of each monomer in the PMMA-RM82 composite polymer formed.

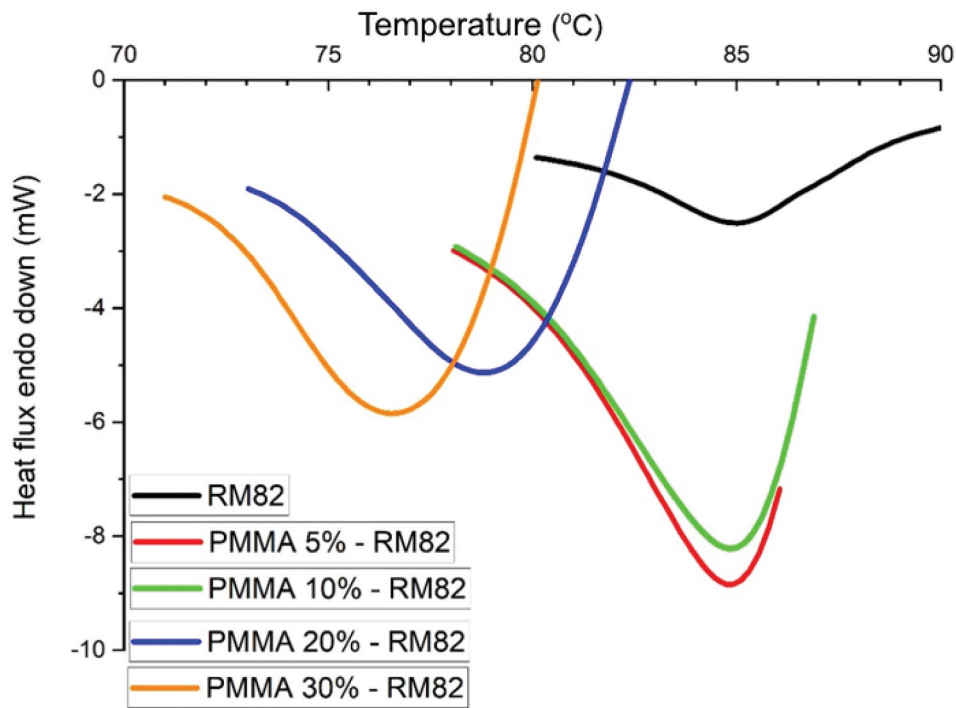The endothermic curve in the RM82 and PMMA-RM82 samples is shown in Figure 5. Endothermic

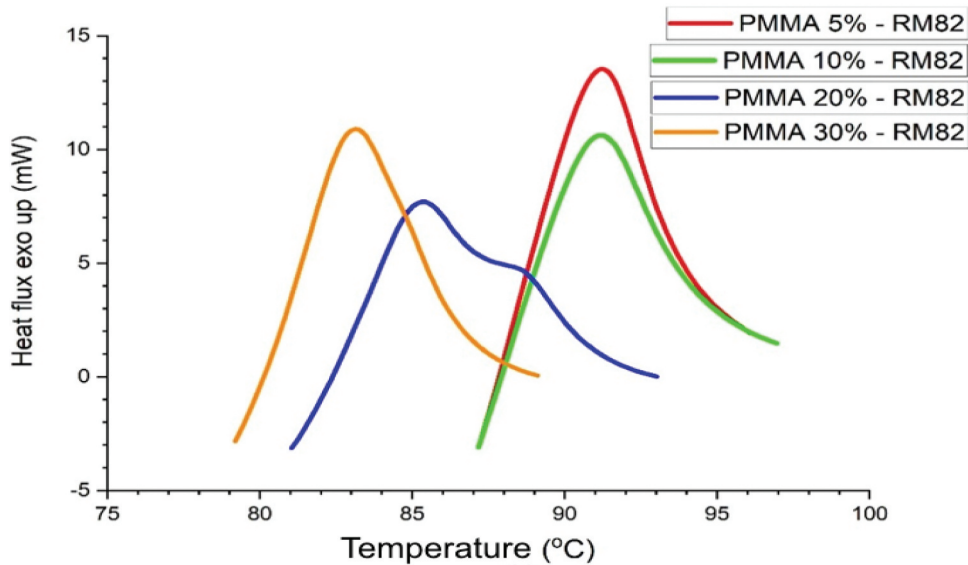**Figure 5.** Endothermic peak curve of PMMA-RM82.

Figure 6. Exothermic peak curve of PMMA-RM82.

activity that occurs is melting. Data for endothermic peaks of composite PMMA-RM82 are presented in Table 1. The RM82 endothermic curve that is formed has a peak at a temperature of 85.01°C and absorbs heat of 59.07 mJ. After adding PMMA, a wide and sharp endothermic peak was produced, which indicates that endothermic activity that occurs in the PMMA-RM82 sample requires greater heat than the RM82 sample [28–30]. After adding PMMA, the polymer undergoes cross-linking in its structure. DSC graphics show a wide and sharp endothermic peak in the PMMA_RM82 sample. This phenomenon indicates that endothermic activity that occurs in the PMMA-RM82 sample requires more heat than in the RM82 sample. Crystallization peaks observed for RM82 endothermic curve show a peak at a temperature of 85.01°C, while for composites PMMA-RM82, they range from about 71.70°C until 78.52°C.

Table 1. Data for endothermic peaks of PMMA-RM82.

Sample	Onset	Peak	Endset	Heat	Enthalpy
RM82	80.47 ℃	85.01 ℃	89.39 ℃	−59.07 mJ	−196.90 J/g
PMMA 5%-RM82	78.52 ℃	84.76 ℃	85.52 ℃	−285.64 mJ	−71.41 J/g
PMMA 10%-RM82	78.15 ℃	84.85 ℃	85.70 ℃	−270.77 mJ	−67.69 J/g
PMMA 20%-RM82	73.27 ℃	78.76 ℃	81.12 ℃	−139.67 mJ	−34.92 J/g
PMMA 30%-RM82	71.70 ℃	76.55 ℃	79.05 ℃	−148.93 mJ	−37.23 J/g

This is indicated by the amount of heat absorbed in the PMMA-RM82 sample, which is more than double the amount of heat absorbed in the RM82 sample. In addition, there was a shift in endothermic temperature peaks in PMMA-RM82 samples, indicating that there was a rapid transformation of thermal activity compared to the thermal transformation of RM82. The amount of PMMA composition in the polymer composites PMMA-RM82 appears to affect their thermal properties, especially when PMMA composition is 20% and 30%. This suggests that MMA monomers at that number form more crosslinking phases in the polymer composites formed.

In the RM82 sample, no significant exothermic activity was detected, and the exothermic peaks data of the composite PMMA-RM82 are presented in Table 2. After melting, there is an increase in heat flux value in the temperature range of 90–100℃, but it does not penetrate the Y-axis (+). The event that occurs is a baseline shift after endothermic activity caused by changes in the mass or specific heat of the sample.

The formation of sloping and wide exothermic-like peaks indicates that the sample is recrystallized but still in the liquid phase. This means that in this temperature range, the sample is actually a liquid but has crystal-like characteristics. In the PMMA-RM82 sample, there was a wide and sharp exothermic curve. The heat released by the PMMA-RM82 sample increased with the increase in PMMA weight percent. This affects the rapid crystallization process of PMMA-RM82, where in PMMA samples 30%-RM82, the heat released is almost twice as much as the heat released by PMMA samples 5%-RM82. The absence of PMMA and RM82 peaks, both endothermic and exothermic, in PMMA-RM82 samples indicates that polymerization has occurred and a new product has formed [13,31–33].

Confirmation of the molecular structure is observed using an FTIR spectrophotometer in Figure 7. The sample is characterized by FTIR with the aim of obtaining information about the emergence of functional groups contained in the sample. Testing of 30% RM82 samples was carried out to obtain preliminary information about functional groups formed in samples without the addition of PMMA.

The FTIR spectrum of RM82 identified more than five absorption bands, which indicate that the sample has a complex structure. Identification at wavenumbers 2939.64 cm^{-1} and 2866.34 cm^{-1} indicates the presence of C-H methyl bond stretching asymmetry (thread). No sharp peaks were detected at wavenumbers between 2000 and 2500 cm^{-1}, indicating that the compound has no triple bond. This is in accordance with the structural drawings of RM82, which do not have triple ties. Furthermore, at wavenumber 1724.44 cm^{-1}, it indicates the presence of a C = O bond conjugate belonging to ketones because no specific peak for aldehydes is found at 2700–2800 cm^{-1}. Furthermore, wavenumbers 1605.81 cm^{-1} and 1512.26 cm^{-1} were identified as C=C aromatic stretching bonds. The presence of an aromatic structure in this data is supported by the appearance of small peaks at 3100–3200 cm^{-1}, which are C-H aromatic stretching bonds. The peaks at wavenumbers 1256.68 cm^{-1} and 1200.74 cm^{-1} indicate C-O ether aromatic stretching bonds, and the peaks in the fingerprint area at wavenumbers around 750–800 cm^{-1}, 850–900 cm^{-1}, and 800–850 cm^{-1} represent C-H substituted 1.2 (ortho), C-H substituted 1.3 (meta), and C-H substituted 1.4 (para) bonds, respectively. Other peaks identified in the fingerprint area are peaks at wavenumber 1411.95 cm^{-1} as C-H methylene bending bonds, wavenumbers 1166.02 cm^{-1} and 1068.61 cm^{-1} as C-O stretching bonds belonging to alkyl substituted ethers, and wavenumber 987.6 cm^{-1} as C-H out-of-plane vinyl with bent vibrations [34–36].

After the addition of PMMA, it was found that the IR spectral form of each variation in the weight percent of PMMA was almost the same, but there was a spectral shift that showed that polymerization had occurred in PMMA-RM82, which was characterized by a reaction to the free radical C=C bond released by the initiator and then reacted with the double bond of the RM82 monomer.

Table 2. Data for exothermic peaks of PMMA-RM82.

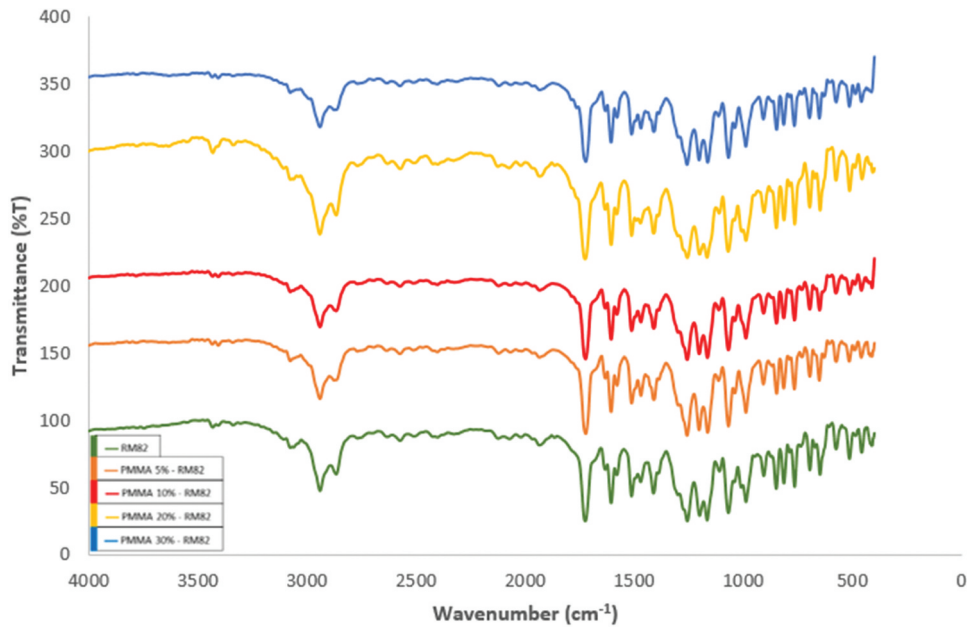| Sample	Onset	Peak	Endset	Heat	Enthalpy
PMMA 5%-RM82	87.21 ℃	91.18 ℃	95.48 ℃	757.79 mJ	189.45 J/g
PMMA 10%-RM82	87.33 ℃	91.24 ℃	96.53 ℃	730.92 mJ	182.73 J/g
PMMA 20%-RM82	81.72 ℃	85.30 ℃	92.78 ℃	1.24 J	309.63 J/g
PMMA 30%-RM82	79.52 ℃	83.11 ℃	88.40 ℃	1.3 J	324.48 J/g

Figure 7. FTIR spectrum of the composite of PMMA-RM82.

Sample testing with XRD aims to obtain information about the diffraction pattern formed in the sample. Sample measurements were carried out at 2θ $5°$–$60°$ at a measurement temperature of 25°C, using Cu anode material (Ka = 1.54060 Å), and the XRD pattern of composite of PMMA-RM82 is illustrated in Figure 8.

The scattering angles for each peak in the XRD pattern of PMMA-RM82 are presented in Table 3 for result identification.

In the RM82 sample, there were sharp peaks at 2θ 10.187°, 20.405°, and 21.627°, with respective peaks intensities being 38,219 a.u., 66,946 a.u., and 23,754 a. u. Sharp peaks with sufficiently high intensity indicate that RM82 has crystalline properties. While in the PMMA-RM82 diffraction pattern, the peaks formed are located at scattering angles similar to RM82, but there is a decrease in intensity as the percent weight of PMMA increases. The decrease in intensity that occurs in
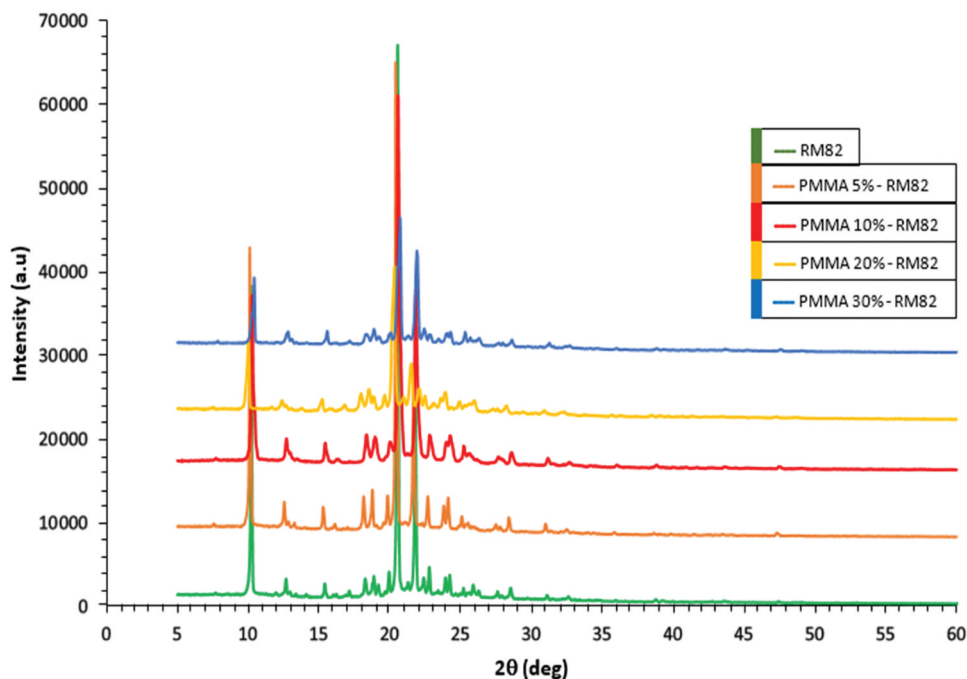

Figure 8. XRD pattern of the composite of PMMA-RM82.

Table 3. Data regarding scattering angles in the XRD pattern of PMMA-RM82.

Sample	Scattering Angle (2θ)
RM82	10.187°
	20.405°
	21.627°
PMMA 5%-RM82	10.068°
	20.26°
	21.508°
PMMA 10%-RM82	10.25°
	20.442°
	21.664°
PMMA 20%-RM82	9.99°
	20.182°
	21.352°
PMMA 30%-RM82	10.38°
	20.572°
	21.742°

PMMA-RM82 samples is in the form of destructive interference, so that the scattered waves will eliminate each other [37]. This decrease in intensity is caused by an increase in the composition of PMMA, which has amorphous properties. Consequently, there is an increase in the amorphous intensity of PMMA, which will decrease the crystallinity of the sample. This is evidenced by the peak intensity in the PMMA-RM82 sample that decreases when the weight percent of PMMA is added to 30%. Generally, polymers have semicrystalline properties because they are polymer chains whose molecular structure is random [38–40].

4. Conclusion

The synthesis process of MMA and liquid crystal RM82 to form composites of PMMA-RM82 involves addition polymerization, also known as free radical polymerization that consists of initiation, propagation, and termination stages. At the initiation stage, the initiator benzoyl peroxide undergoes homolytic breaking at high temperatures, producing benzoyl radicals. Furthermore, at the propagation stage, the benzoyl radical attacks the reactive mesogen monomer RM82 and MMA monomer, and it is expected that the two monomers combine to form a long chain of polymers. The morphology of composites polymer PMMA-RM82 appears transparent, and at higher concentrations of MMA, the surface of the composites appears opaque. Based on the SEM images, it can be seen that the surface of composites PMMA-RM82 that when the sample began to add PMMA, which is with a PMMA weight percent of 5%, there is a new shape in the form of a large circle attached to the end of the blade. The thermal analysis showed that the DSC curve for RM82 only has small endothermic peaks and are not very sharp, while the DSC curve for PMMA-RM82 has sharp endothermic and exothermic peaks. This indicates that

the thermal transformation activity of RM82 tends to be slow, with a small enthalpy change at peak, whereas after the addition of PMMA at a certain weight percent, there is a rapid thermal transformation activity, with a large enthalpy change compared to enthalpy change without PMMA addition.

Disclosure statement

No potential conflict of interest was reported by the author(s).

ORCID

Afrizal http://orcid.org/0000-0003-0334-5111

References

[1] Hussein MA, Abdel-Rahman MA, Asiri AM, et al. Review on: liquid crystalline polyazomethines polymers. Basics, syntheses and characterization. Des Monomers Polym. 2012;15(5):431–463. doi: 10.1080/1385772X.2012.688325

[2] Al Sheheri SZ, Al-Amshany ZM, Al Sulami QA, et al. The preparation of carbon nanofillers and their role on the performance of variable polymer nanocomposites. Des Monomers Polym. 2019;22(1):8–53. doi: 10.1080/15685551.2019.1565664

[3] Atabaki F, Shokrolahi A, Pahnavar Z. Methyl methacrylate based copolymers and terpolymers: preparation, identification, and plasticizing capability for a poly (methyl methacrylate) used in aviation. J Appl Polym Sci. 2018;135(34):1–13. doi: 10.1002/app.46603

[4] Jafarpour M, Aghdam AS, Koşar A, et al. Electrospinning of ternary composite of PMMA-PEG-SiO2 nanoparticles: comprehensive process optimization and electrospun properties. Mater Today Commun. 2021 June;29:102865. doi: 10.1016/j.mtcomm.2021.102865

[5] Li Y, Luo D. Fabrication and application of 1D micro-cavity film made by cholesteric liquid crystal and reactive mesogen. Opt Mater Express. 2016;6(2):691. doi: 10.1364/OME.6.000691

[6] Chen F, Cong Y, Zhang B. Synthesis and characterization of liquid crystalline epoxy with cholesteric structure for modification of epoxy resin. Des Monomers Polym. 2016;19(6):560–568. doi: 10.1080/15685551.2016.1187441

[7] Kloos J, Joosten N, Schenning A, et al. Self-assembling liquid crystals as building blocks to design nanoporous membranes suitable for molecular separations. J Memb Sci. 2021;620(September 2020):118849. doi: 10.1016/j.memsci.2020.118849

[8] Fan Z, Gong F, Nguyen ST, et al. Advanced multifunctional graphene aerogel - poly (methyl methacrylate) composites: experiments and modeling. Carbon N Y. 2015;81(1):396–404. doi: 10.1016/j.carbon.2014.09.072

[9] Afrizal A, Budi S, Yusmaniar Y, et al. Photopolymerization of Monomer Methyl Methacrylate (PMMA) with Indium Tin Oxide (ITO) nanoparticle and modifications by polyethylene-block-polyethylene glycol (PE-B-PEG) using UV curing technology. Rasayan J Chem. 2022;15(3):1990–1996. doi: 10.31788/RJC.2022.1537014

[10] Ali U, Karim KJBA, Buang NA. A review of the properties and applications of poly (Methyl Methacrylate) (PMMA). Polym Rev. 2015;55(4):678–705. doi: 10.1080/15583724.2015.1031377

[11] Ullah MW, Haraguchi N, Ali MA, et al. Synthesis of homo- and copolymer containing sulfonic acid via atom transfer radical polymerization. Des Monomers Polym. 2022;25(1):261–270. doi: 10.1080/15685551.2022.2126092

[12] Minami H, Kagawa Y, Kuwahara S, et al. Dispersion atom transfer radical polymerization of methyl methacrylate with bromo-terminated poly(dimethylsiloxane) in supercritical carbon dioxide. Des Monomers Polym. 2004;7(6 SPEC. ISS.):553–562. doi: 10.1163/1568555042474103

[13] Barim G, Yayla MG, Degirmenci M. Copolymerization of cyclohexene-3-yl methyl methacrylate with styrene: synthesis, characterization, monomer reactivity ratios, and thermal properties. Des Monomers Polym. 2014;17(7):610–616. doi: 10.1080/15685551.2014.907613

[14] Arslan Z, Kiliclar HC, Yagci Y. Dimanganese decacarbonyl catalyzed visible light induced ambient temperature depolymerization of poly(methyl methacrylate. Des Monomers Polym. 2022;25(1):271–276. doi: 10.1080/15685551.2022.2135730

[15] Wu J, Zhao Z, Hamel CM, et al. Evolution of material properties during free radical photopolymerization. J Mech Phys Solids. 2018;112:25–49. doi: 10.1016/j.jmps.2017.11.018

[16] O'Donnell AD, Salimi S, Hart LR, et al. Applications of supramolecular polymer networks. React Funct Polym. 2022;172:105209. doi: 10.1016/j.reactfunctpolym.2022.105209

[17] Kloos J, Jansen N, Houben M, et al. On the order and orientation in liquid crystalline polymer membranes for gas separation. Chem Mater. 2021;33(21):8323–8333. doi: 10.1021/acs.chemmater.1c02526

[18] Qu M, Nilsson F, Schubert DW. Effect of filler orientation on the electrical conductivity of carbon fiber/PMMA composites. Fibers. 2018;6(1):1–10. doi: 10.3390/fib6010003

[19] Lin X, Gablier A, Terentjev EM. Imine-based reactive mesogen and its corresponding exchangeable liquid crystal elastomer. Macromolecules. 2022;55(3):821–830. doi: 10.1021/acs.macromol.1c02432

[20] Plamont R, Lancia F, Ryabchun A. Reactive mesogens for ultraviolet-transparent liquid crystal polymer networks. Liq Cryst. 2020;47(11):1569–1581. doi: 10.1080/02678292.2020.1749902

[21] Di Mauro A, Farrugia C, Abela S, et al. Ag/ZnO/PMMA nanocomposites for efficient water reuse. ACS Appl Bio Mater. 2020;3(7):4417–4426. doi: 10.1021/acsabm.0c00409

[22] Mahani AA, Motahari S, Nayyeri V. Electromagnetic and microwave absorption characteristics of PMMA composites filled with a nanoporous resorcinol formaldehyde based carbon aerogel. RSC Adv. 2018;8(20):10855–10864. doi: 10.1039/C8RA00196K

[23] Al-Hamdan RS, Almutairi B, Kattan HF, et al. Influence of hydroxyapatite nanospheres in dentin adhesive on the dentin bond integrity and degree of conversion: a scanning electron microscopy (SEM), Raman, Fourier transform-infrared (FTIR), and microtensile study. Polymers. 2020;12(12):1–15. doi: 10.3390/polym12122948

[24] Wang T, Sun Z, Liang F, et al. Poly(methylmethacrylate) microspheres with matting characteristic prepared by dispersion polymerization. Int J Polym Anal Charact. 2019;24(8):731–740. doi: 10.1080/1023666X.2019.1670393

[25] Feng X, Kawabata K, Kaufman G, et al. Highly selective vertically aligned nanopores in sustainably derived polymer membranes by molecular templating. ACS Nano. 2017;11(4):3911–3921. doi: 10.1021/acsnano.7b00304

[26] Marin San Roman P, Nijmeijer K, Sijbesma RP. Sulfonated polymerized liquid crystal nanoporous membranes for water purification. J Memb Sci. 2022;644(November 2021):120097. doi: 10.1016/j.memsci.2021.120097

[27] Takagi H. Review of functional properties of natural fiber-reinforced polymer composites: thermal insulation, biodegradation and vibration damping properties. Adv Compos Mater. 2019;28(5):525–543. doi: 10.1080/09243046.2019.1617093

[28] PerkinElmer. Differential scanning calorimetry beginner's guide. 2013.

[29] Ibrahim Y, Elkholy A, Schofield JS, et al. Effective thermal conductivity of 3D-printed continuous fiber polymer composites. Adv Manuf Polym Compos Sci. 2020;6(1):17–28. doi: 10.1080/20550340.2019.1710023

[30] Shyly PM, Ammakutti Sridevi N, Sumithraj Premkumar P. Thermal and mechanical studies of nanochitosan incorporated polymethyl methacrylate-based composite electrolytes. J Eng Appl Sci. 2022;69(1):1–14. doi: 10.1186/s44147-022-00077-5

[31] Saxena P, Shukla P, Gaur MS. Thermal analysis of polymer blends and double layer by DSC. Polym Polym Compos. 2021;29(9):S11–S18. doi: 10.1177/0967391120984606

[32] Chmela Š, Fiedlerová A, Liptaj T, et al. Synthesis and homopolymerization kinetics of 7-(methacroyloxy)-

2-oxo-heptylphosphonic acid and its copolymerization with methyl methacrylate. Des Monomers Polym. 2019;22(1):79–90. doi: 10.1080/15685551.2019.1582216

[33] Krishnasamy S, Thiagamani SMK, Muthu Kumar C, et al. Recent advances in thermal properties of hybrid cellulosic fiber reinforced polymer composites. Int J Biol Macromol. 2019;141:1–13. doi: 10.1016/j.ijbiomac.2019.08.231

[34] Alsulami QA, Rajeh A. Structural, thermal, optical characterizations of polyaniline/polymethyl methacrylate composite doped by titanium dioxide nanoparticles as an application in optoelectronic devices. Opt Mater (Amst). 2022;123:111820. doi: 10.1016/j.optmat.2021.111820

[35] Yang W, Rallini M, Wang DY, et al. Role of lignin nanoparticles in UV resistance, thermal and mechanical performance of PMMA nanocomposites prepared by a combined free-radical graft polymerization/masterbatch procedure. Compos Part A Appl Sci Manuf. 2018;107:61–69. doi: 10.1016/j.compositesa.2017.12.030

[36] Jaikumar V, Kumar D. New UV-Curable prepolymer: synthesis, characterization, and kinetics analysis. Int J Polym Anal Charact. 2015;20(6):481–490. doi: 10.1080/1023666X.2015.1050629

[37] Yogeswari C, Sabari Girisun TC, Nagalakshmi R. Electrospun 2-nitroaniline (2NA) – poly (methylmethacrylate) (PMMA) nanofibers for power limiting and Q-switching applications. Chem Phys Lett. 2022;786 (November):139209. doi: 10.1016/j.cplett.2021.139209

[38] Hafeez A, Akhter Z, Gallagher JF, et al. Liquid phase synthesis of aromatic poly(azomethine)s, their physicochemical properties, and measurement of ex situ electrical conductivity of pelletized powdered samples. Des Monomers Polym. 2017;20(1):74–88. doi: 10.1080/15685551.2016.1231042

[39] Neto JSS, de Queiroz HFM, Aguiar RAA, et al. A review on the thermal characterisation of natural and hybrid fiber composites. Polymers. 2021;13(24):4425. doi: 10.3390/polym13244425

[40] Rahaman MH, Yaqoob U, Kim HC. The effects of conductive nano fillers alignment on the dielectric properties of copolymer matrix. Adv Manuf Polym Compos Sci. 2019;5 (1):29–36. doi: 10.1080/20550340.2019.1567067